Study of Cadmium Complexation with Na-DDTC by Voltammetry and Spectrophotometric Method and its Application in Corrosion Inhibition

Djamila Hammoum, Lahcène Larabi* and Yahia Harek

Laboratory of Analytical Chemistry and Electrochemistry, Department of Chemistry, Tlemcen University, Tlemcen, Algeria
*Corresponding author: larabi_lahcene@yahoo.fr

Received 20/01/2024; accepted 18/04/2024
https://doi.org/10.4152/pea.2026440104

Abstract
Stoichiometry and β of Cd(II)/Na-DDTC complex were herein determined by DPV, employing Lingane's equation in a simple and extended form. Ionic strength was kept constant by using $NaClO_4$ and KNO_3 as SE. All measurements were performed at a constant T of 298±1 K. The approximation of all possible Lingane's equations was established. According to obtained results, it was concluded that the equation should be used in its extended form. In KNO_3 and in $NaClO_4$, q was found to be 5 and 6, and β logarithms were found to be 21.20 and 24.47, respectively. Spectrophotometric study was also performed to determine stoichiometry and β of Cd(II)/Na-DDTC complex in the same SE. Data indicated that Na-DDTC should be combined with Cd in molar ratios of 1:5 (ML_5), in KNO_3, and of 1:6 (ML_6), in $NaClO_4$. β logarithms were calculated to be 22.26 and 23.94, in KNO_3 and $NaClO_4$, respectively. IE(%) of Na-DDTC as an ecofriendly CI for CS in 0.5 M H_2SO_4 medium was also investigated using WL measurements. Experimental results showed that IE(%) increased with higher inhibitor's Ct. The inhibitor's adsorption onto the CS surface obeyed Langmuir's isotherm, and it proceeded by both physisorption and chemisorption modes. ΔG_{ads} was determined. The effect of Cd^{2+} addition, which formed a complex with Na-DDTC, was also studied.

***Keywords*:** β; CI; DPV; Job's method; Na-DDTC.

Introduction•

A broad range of complexes used in industries, pharmaceutical processes, agriculture and medicinal chemistry has garnered significant interest in recent years. DTC are a class of organic chemicals that have been extensively used in the field of fine organic synthesis, particularly in the production of pesticides, herbicides and fungicides [1]. Due to the elevated electron density of S atom in these ligands, and to the existence of active sites with C=S and C-S bonds, DTC are able to create insoluble complexes, and provide stability to metal ions in various oxidation states [2-4]. Recently, it has been found that metal-DTC complexes enhance cytotoxic action mechanisms [5-7], and are able to stimulate the growth of tumor cells [8, 9].

•The abbreviations and symbols definition lists are in pages 62-64.

Furthermore, they have been employed as chemotherapeutic agents. DTC also hinders the corrosion process, due to the existence of N and S as electronegative elements [10]. The substance is adsorbed onto the metal surface, creating a protective layer that prevents corrosion, at certain areas [11]. Recent studies have shown that Na-DDTC is a very effective, secure and cost-effective CI for metals in aggressive environments [12-16]. [12] have assessed the IE(%) of Na-DDTC on CS corrosion in a HCl solution, by employing Tafel polarization and electrochemical impedance techniques. Data indicated that the ligand was an effective CI, despite its tendency to expedite the anodic process.

Various analytical approaches are employed to synthesize, analyze and characterize these substances. Electrochemical analysis is a crucial method for characterizing DTC complexes. This methodology has several key benefits, including rapid analysis speed [17], excellent selectivity and sensitivity, a low detection limit, relative simplicity and less equipment costs than those of other methods [18, 19]. Additionally, its reproducibility is enhanced by the use of a renewable surface electrode [20]. Among these electroanalytical approaches, polarography is widely regarded as a productive and adaptable technique to investigate complexes in solutions. For many metal-ligand systems, it is possible to determine the degree of formation, distribution and β of all species present [21].

In continuation of previous researches in the field by the authors of this study, Na-DDTC was herein used as a ligand to coordinate with Cd ion. Its general chemical formula is $C_5H_{10}NS_2Na$. Na-DDTC's chemical structure is shown in Scheme 1.

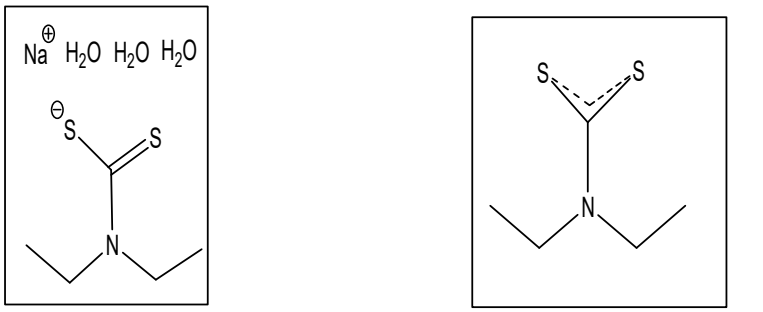

Sodium diethyldithiocarbamate trihydrate ionic diethyldithiocarbamate

Scheme 1: Molecular structure of Na-DDTC.

Herein, β and stoichiometry of Cd-Na-DDTC complex were calculated, by using classical and extended Lingane's equations in two different SE (KNO_3 and $NaClO_4$). Then, the results were compared to those of spectrophotometric techniques like Job's method. Finally, the complex was employed as CI for CS in a H_2SO_4 medium.

Materials and methods

Stock solutions preparation

$NaClO_4$ was obtained from Fluka. KNO_3, Cd and $CdCl_2H_2O$ (Fw: atomic absorption standard (98%) were purchased from Aldrich.

The 5.10^{-3} M Cd^{2+} reference solution was prepared by weighing out the required amount of $CdCl_2H_2O$ and dissolving it in 100 mL Milli-Q® water.
The 10^{-5} M Cd^{2+} solution used in this study was prepared by diluting 5.10^{-3} M Cd^{2+} with 10 mL 0,1 M KNO_3 or 0,1 M $NaClO_4$ in the polarographic cell.
Na-DDTC (Fw: 225.331) was purchased from Sigma Aldrich. Na-DDTC solutions with Ct from 1.10^{-4} to 3.10^{-4} M were prepared by weighing out their required amounts and dissolving them in the same solution of 0.1 M KNO_3 or 0.1 M $NaClO_4$, as those used for preparing the Cd^{2+} solution.
H_2SO_4 (Fw: 98.08, purity of 99.99%) used in WL measurements was purchased from Sigma Aldrich.

Equipments
DPV measurements were performed using a Trace-Lab50 from Radiometer, which included a polarographic analyser (Pol150) and stand (MDE150), monitored by Trace Master 5 software. These measurements were carried out using a conventional three-electrode system. The working electrode was a HMDE, with a capillary diameter of 70 µm. Potential's values were expressed *vs.* an Ag/AgCl (3 M KCl) electrode separated from the test solution by a salt bridge containing the solvent/SE. The auxiliary electrode was a Pt wire.
Spectrophotometric measurements were performed on a UV-visible Thermo Electron Corporation Nicolet Evolution 100 device, using a matched 10 mm quartz cell.
The pH measurements were carried out employing a pH-meter from Denver Instrument Company.

Electrochemical method
In DPV experiments, the pulse duration was programmed to 0.04 s, and the scan rate was 125 mV/s. Initial and final potential's values were -400 and -700 mV, respectively. A 10 mL SE was placed in the polarographic cell. A magnetic stirrer provided the convective transport. Pure N^2 was bubbled through the experimental solution to remove dissolved O^2. Data were analyzed using Lingane's equations.

Lingane's equation
For the reaction denoted as $M^{m+} + qL \rightarrow (MLq)^{m+}$ (where M is a metal with a charge of m^+ and L is a neutral ligand with a stoichiometric coefficient of q), the polarographic half wave or E_p shifts more negatively with higher Ct of Na-DDTC added to Cd ion solution. Lingane's [22] classical equation is derived in Eq. (1), to calculate β, when activity coefficients were not considered.

$$\Delta E_p = \frac{2.303RT}{nF}\log\beta + q\frac{2.303RT}{nF}\log C_L \qquad (1)$$

where n value of was = 2. This equation has been successfully applied by several researchers for determining β and the ligand's stoichiometric coefficient complexation reactions [22, 23].

Extended Lingane's equation
If the current's effect is included, the classical Lingane's equation should be extended as follows [24, 25] in Eq. (2):

$$\Delta E_p = \frac{2.303RT}{nF} log\,[\frac{I_{MLq}}{I_M}\frac{\gamma_M\gamma_L^q}{\gamma_{MLq}}\beta_{M\gamma_L^q}C_L^q] \quad (2)$$

This equation can only be applied when the system involves a complex highly stable.

Spectrophotometric method

For determining stoichiometry and K_f, A of a series of metal salt and ligand mixtures was initially measured at 298 K. Then, in order to perform β variation with changes in T, A shifts at different T were studied.

Data were analyzed using Job's method, also called CVM, which was selected, since it is easy, simple and commonly employed [26] to determine anions and organometallic compounds, and to help understand ligands/metal action modes [26-28]. In analytical chemistry, it is mainly used to determine the stability of a complex, its K_f and composition. Optical measurements were employed to study a system with two or three components.

The procedure included making a volume of 2 mL metal complex solutions with different Ct of Cd ions and ligands (Table 1).

Table 1: Metal complex solutions containing different Ct of Cd ions and ligands.

Sr. no of solution	1	2	3	4	5	6	7	8	9	10	11
Cd ion volume (mL)	0.0	0.2	0.4	0.6	0.8	1.0	1.2	1.4	1.6	1.8	2.0
Na-DDTC volume (mL)	2.0	1.8	1.6	1.4	1.2	1.0	0.8	0.6	0.4	0.2	0.0

Then, the sum of the Ct from Cd^{2+} was calculated by Eq. (3):

$$C_L + C_M = Ct \text{ (constant)} \quad (3)$$

The optical densities of the solutions, prepared in the previous step, were determined at the wavelength of a light strongly absorbed by Cd-Na-DDTC. The metal-ion and the ligand did not absorb at this wavelength.

A was plotted against f_L (= C_L /Ct). This plot is referred to as a Job's plot. For calculating the Ct of Cd-Na-DDTC, Eq. 3 was rewritten as Eq. (4):

$$\frac{C_M}{Ct} + \frac{C_L}{Ct} = 1 \quad (4)$$

Since, as in Eq. (5):

$$\frac{C_L}{Ct} = f_L \quad (5)$$

Eq. (4) can be reduced to Eq. (6):

$$\frac{C_M}{Ct} = 1 - f_L \quad (6)$$

From Eqs. (5) and (6) q can be obtained in Eq. (7):

$$q = \frac{C_L}{C_M} = \frac{f_L}{1-f_L} \quad (7)$$

Job's diagram, as shown in Fig. 6, consists of two straight lines intersecting at A_0, at a given value of f_L, which indicates Cd:Na-DDTC ratio in ML_q.

Once q was determined, K_f was calculated [29, 30] by Eqs. (8) and (9):

$$M + qL \leftrightarrow ML_q \quad (8)$$

$$K_f = \frac{[ML_q]}{[M][L]^q} \quad (9)$$

A was plotted at λ_{max} *vs*. f_L, in order to obtain Job's diagram. A and f_L were given by Eqs. (10) and (11):

$$A = A_{ML} - (\varepsilon_L C_L + \varepsilon_M C_M) \quad (10)$$

$$f_L = \frac{C_L}{(C_M + C_L)} \quad (11)$$

The deviation from A_o values was due to Cd-Na-DDTC's complex dissociation. Thus, β was determined from theoretical lines deviations (Fig. 6). A_{max} denoted A value at the highest point on the experimental curve, indicating the maximum amount of the complex formed with a dissociation degree (α). A_o represents absorbance value, where the theoretical straight lines intersected due to the complex, when its maximum Ct was formed, with a value of α = 0. A_α represents the absorbance value of the complex's dissociated part, which is the difference between A_0 and A_{max}. In order to quantify β, it was imperative to determine α, which was calculated by employing Eq. (12):

$$\alpha = \frac{A_0 - Amax}{A_0} \quad (12)$$

At equilibrium, Eq. (13) is as follows in Eq. (14):

$$C_{MLq} = (1-\alpha)C \; ; \; C_M = \alpha C \; ; C_L = q\alpha C \quad (13)$$

So, K_f was given by:

$$K_f = \frac{(1-\alpha)}{q^q \times \alpha^{q+1} \times c^q} \quad (14)$$

CI study

Corrosive solution

0.5 M H_2SO_4 was used as an aggressive solution, prepared by diluting a 99.99% analytical reagent grade with ultra-pure water.

For WL measurements, 100 mL of the test solution were used, and the Ct of the studied inhibitors varied from 50 to 500 mg/L.

WL measurements

Rectangular samples of CS XC38 (AFNOR/Euronorm: C35E CS and US specification: SAE1035), of 3 × 1.4 × 0.25 cm, were obtained by cutting plates with the chemical composition (wt.%): C = 0.37%, S = 0.016%, Cr = 0.077%, Mn = 0.68%, Si = 0.23%, Ti = 0.011%, Ni = 0.059%, Co = 0.009%, Cu = 0.160% and remainder iron (Fe), which were used for WL measurements. The samples were gradually polished with 200 to 1200 grade emery paper, with a pitch of 200. They were rinsed with double distilled water, degreased, washed thoroughly with double distilled water, dried in a stream of hot air, and weighed. Then they were immersed

in the test aggressive solution without and with inhibitor, at different Ct, for 1 h, at T in the range from 298 to 323 K. At the end of the test period, the samples were withdrawn, cleaned with water, dried and reweighed. All measurements were repeated at least thrice, to ensure the results reproducibility.
The measured CR (mg/cm^{-2}/h) was determined using Eq. (15):

$$v = \frac{m_0 - m_1}{At} \quad (15)$$

where m_0 and m_1 are the weight of samples before and after immersion, respectively, t is immersion time (1 h) and A is the samples' total exposed surface area.
According to several authors [31-33], IE(%) may be calculated using Eq. (16):

$$\text{IE}(\%) = \frac{v_0 - v}{v_0} \times 100 \quad (16)$$

where v_0 and v denote average WL in a H_2SO_4 solution without and with inhibitor, respectively.

Results and discussion

Voltammetric behavior

β of Cd-Na-DEDTC complex was calculated by DPV. KNO_3 and $NaClO_4$ solutions were tested as SE, with an ionic strength of 0.1 M, at 298 K.
Under these conditions, 10^{-5} M Cd^{2+} showed a peak at about -500 mV, without the ligand. With Na-DEDTC added, at different Ct, to the Cd ion, its E_p shifted towards more negative values than those of the simple and free states. DPV values of Cd^{2+} in different Ct of Na-DDTC are shown in Figs. 1 and 2.

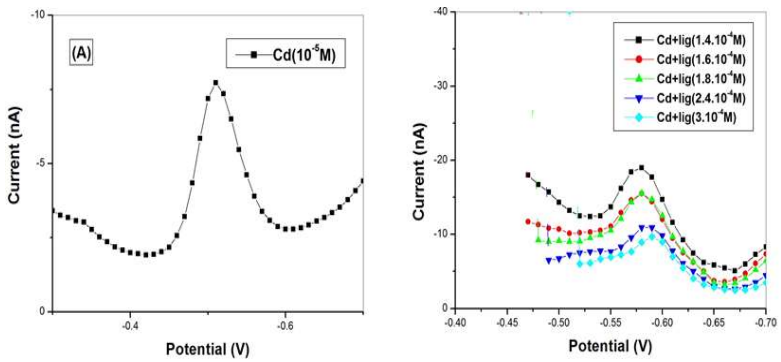

Figure 1: DPV of- **(A)** 10^{-5} M Cd^{2+} and **(B)** different Ct of Na-DDTC in 0.1 M $NaClO_4$.

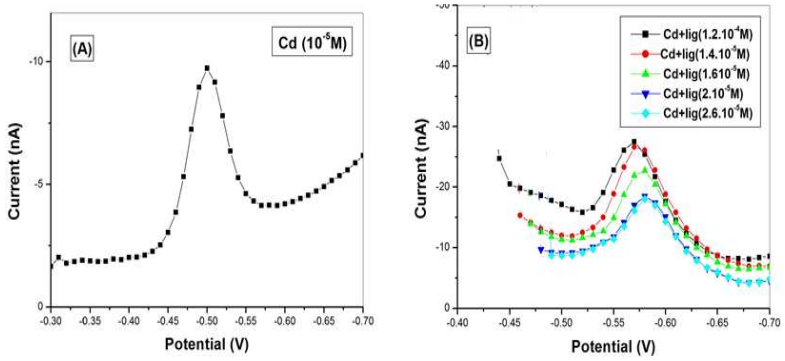

Figure 2: DPV **(A)** without and **(B)** with Na-DDTC, at different Ct in 0.1 M KNO_3.

This significant displacement was used to determine β and q, using simple and extended Lingane's equations. The obtained results are listed in Tables 2 and 3.

Table 2: ΔE_p *vs.* Ag/AgCl and peak current of a 10^{-5}M Cd^{2+} solution as a function of the Ct from Na-DDTC with 0.1 M $NaClO_4$.

Ct of Na-DDTC (M) x 10^4	E_p (V)	I_p (nA)	logC_L	logI_M/I_{ML}	ΔE_p (V)	A_L x 10^5 (M)	logA_L
0	0.52	5.763					
1.4	0.57	14.864	3.853	-0.411	0.05	9.99	4.000
1.6	0.58	11.843	3.795	-0.312	0.06	11.42	3.942
1.8	0.59	11.268	3.744	-0.291	0.07	12.85	3.891
2.4	0.60	7.866	3.619	-0.135	0.08	17.13	3.766

Table 3: ΔE_p *vs.* Ag/AgCl and peak current of a 10^{-5} M Cd^{2+} solution as a function of the Ct from Na-DDTC with 0.1 M KNO_3.

C_L x 10^4 (M)	E_p (V)	Ip (nA)	logC_L	logI_M/I_{ML}	ΔE_p (V)	A_L x 10^5 (M)	logA_L
0	0.51	9.798					
1.2	0.56	27.510	3.920	-0.448	0.05	8.56	4.067
1.4	0.57	26.310	3.853	-0.428	0.06	9.99	4.000
1.6	0.58	22.680	3.795	-0.364	0.07	11.42	3.942
2.0	0.59	18.610	3.698	-0.278	0.08	14.28	3.845
2.6	0.60	17.00	3.585	-0.239	0.09	18.56	3.731

β values of Cd-Na-DDTC complex obtained from Eq. 1 were equal to 17.52 for KNO_3 and 20.2 for $NaClO_4$. The values of q were 4 in KNO_3 and 5 in $NaClO_4$. The values obtained from Eq. 2 for logβ were 21.20 and 24.48, in KNO_3 and $NaClO_4$, respectively. Those of q were 5 in KNO_3 and 6 in $NaClO_4$. Thus, it is noted that there was a significant difference in the results obtained by Eqs. (1) and (2), which seems to be due to the change in peak intensity.

Validity of approximation

In this step, the same approximations that were used by [34] were adopted. Lingane's equation was applied by considering Na-DDTC's activity instead of its Ct. Ionic strength was considered 0.1 M, and the ligand's activity coefficient was found to be 0.714. Thus, obtained results are given in Table 4, which shows that logβ on KNO_3 and $NaClO_4$ originated errors of -0.75 and -3.59%, respectively. Concerning q, on KNO_3 and $NaClO_4$, 0.064% and 0.00%, respectively, were obtained. That is why it was concluded that Lingane's equation should be used in its extended form, and that the approximation $\gamma_M x \gamma_L^q/\gamma_{ML} = 1$ was not favorable. Thus, and still in agreement with [34], q and logβ values were obtained by plotting $n\Delta E_p/0.059 + \log(I_M/I_{ML})$, as an activity's function (Fig. 3). In this context, even if ΔE_p remains constant, β and q can be calculated by plotting $\log(I_M/I_{ML})$ as log CL's function [35].

Cd^{2+} reversibility in Na-DDTC presence was verified by DPV. As Fig. 4 shows, according to $E_{pa} - E_{pc}$, values were close to 30 mV, and to I_{pa}/I_{pc}, were near to unity. This indicated that the system, including the cation with Na-DDTC, was reversible. A similar result was found by [36], who have studied complexation reactions of Zn^{2+}, Pb^{2+}, Cd^{2+} and $T1^{+}$ metal cations by 5,7- diiodo-8-hydroxyquinoline in non-aqueous solvents.

Table 4: Results of q and logβ determination for Cd-Na-DDTC calculated from DPV at 298 K.

Extended Lingane's equations	KNO_3			$NaClO_4$		
	q	log β_N	R^2	q	log β_N	R^2
$n.\Delta E_p/0.0591 + log\frac{I_M}{I_{ML}} = f(\log C_L)$	4.94	21.20	0.988	6.005	24.47	0.982
$n.\Delta E_p/0.0591 + log\frac{I_M}{I_{ML}} = f(\log a_L)$	4.94	21.36	0.988	6.005	25.35	0.982

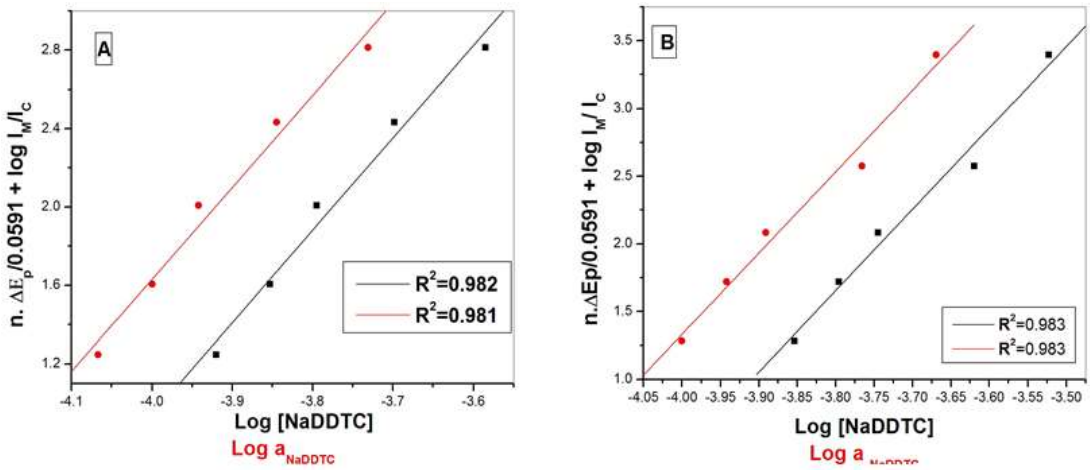

Figure 3: Linear dependence of ΔE_p on Na-DDTC activity and C_L in - **(A)** KNO_3 and **(B)** $NaClO_4$.

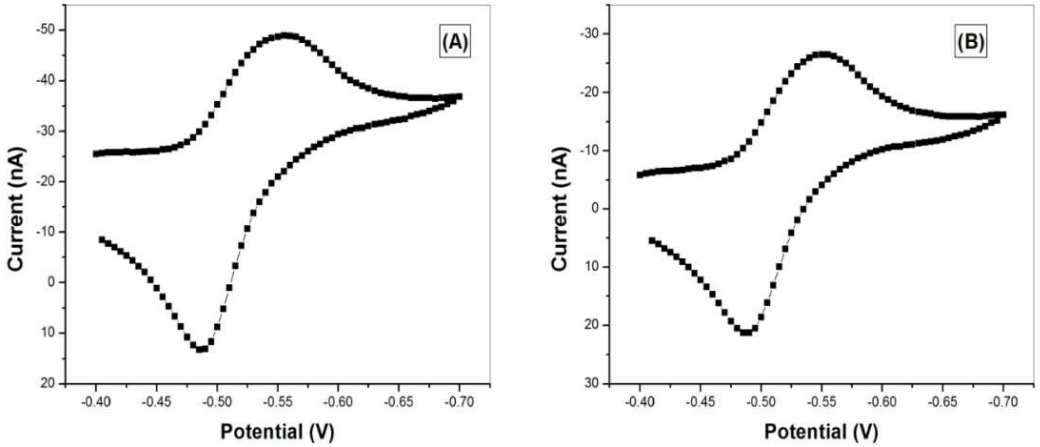

Figure 4: DPV of 10^{-5} M Cd^{2+} with 10^{-4} M Na-DDTC in- **(A)** 0.1 M KNO_3 and **(B)** 0.1 M $NaClO_4$; scan rate of 125 mV/s, at 25 °C.

Spectrophotometric behavior

The obtained results of β and q in both SE were checked using spectrophotometric technique. Electronic spectra of Na-DDTC and Cd(II) complex in KNO_3 are shown in Fig. 5. When Cd^{2+} ion was added to Na-DDTC in the KNO_3 solution, two absorption peaks were seen. The first, at λ_{max} = 256 nm, corresponds to n-π transition of S-C=S, and the second, at λ_{max} = 280 nm, is assigned to the intraligand π-π* transition of N-C-SS. S absorption was determined [37, 38]. In perchlorate salts, the first absorption peak appeared in the same place, while a 20 nm bathochromic shift occurred at 300 nm.

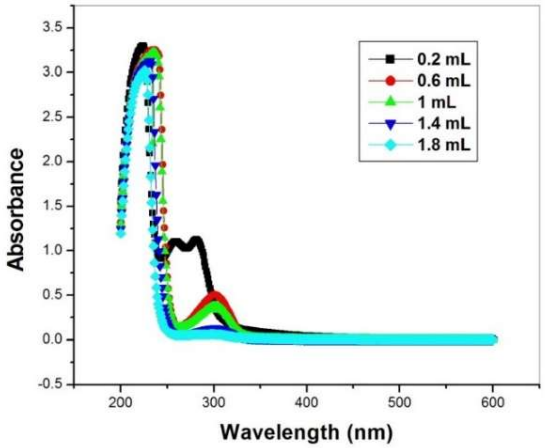

Figure 5: Cd-Na-DDTC absorption spectra in a solution with decreasing Na-DDTC, increasing CS and constant total Ct in 0.1 M $NaClO_4$, at 298±0.1 K.

According to the results in Tables 5 and 6, Job's diagrams were drawn by plotting absorbance as f_L function, at 280 nm and 300 nm, in KNO_3 and $NaClO_4$ solutions, respectively. β and q were derived from Eqs. (7) and (14).

Table 5: Spectrophotometric data for Cd-Na-DDTC system in the 0.1 M KNO_3 solution, with pH of 7.5, at different T.

$[Cd^{2+}]$ x 10^5 (M)	[Na-DDTC] x 10^5 (M)	$\frac{C_L}{(C_M + C_L)}$	A (λ_{max} = 280 nm)		
			298 K	313 K	323 K
0	10.0	1	-	-	-
0.5	9.5	0.95	0.597	0.542	0.516
1.0	9.0	0.9	0.606	0.525	0.487
1.5	8.5	0.85	0.915	0.843	0.796
2.0	8.0	0.8	0.870	0.828	0.801
3.0	7.0	0.7	0.794	0.709	0.654
5.0	5.0	0.5	0.552	0.483	0.441
6.0	4.0	0.4	0.538	0.468	0.425
7.0	3.0	0.3	0.35	0.21	0.188
8.0	2.0	0.2	0.262	0.216	0.215
9.0	1.0	0.1	0.135	0.129	0.109
10.0	0	0	-	-	-

Table 6: Spectrophotometric data for Cd-Na-DDTC system in the 0.1 M $NaClO_4$ solution, with pH = 7.5, at different T.

$[Cd^{2+}]$ x 10^5 (M)	[Na-DDTC] x 10^5 (M)	$\frac{C_L}{(C_M + C_L)}$	A (λ_{max} = 300 nm)		
			298 K	313 K	323 K
0	10.0	-	-	-	-
0.5	9.5	0.95	0.123	0.196	0.205
1.0	9.0	0.9	0.277	0.302	0.304
1.5	8.5	0.8	0.502	0.496	0.604
2.0	8.0	0.85	0.554	0.538	0.582
2.5	7.5	0.75	0.519	0.534	0.573
3.0	7.0	0.7	0.505	-	-
5.0	5.0	0.5	0.334	0.376	0.38
6.0	4.0	0.4	0.213	-	-
7.0	3.0	0.3	0.129	0.169	0.231
8.0	2.0	0.2	0.129	0.166	0.179
9.0	1.0	0.1	0.06	0.101	0.103
10.0	0	0	-	-	-

Fig. 6 depicts Job's diagram in $NaClO_4$, showing that the straight lines intersected at $f_L = 0.85$, which indicates that Cd^{2+} coordinated with six Na-DDTC ligands. The same was seen for KNO_3. In this case, q was found to be 5. All measurements were taken at a pH of 7.5, since Na-DDTC was dissolved in acidic media. These results can be compared with those obtained by DPV. In addition, in this area, hydroxyl groups formation was suppressed. When the results obtained in both SE were compared, it was found that β in KNO_3 was lower than that in $NaClO_4$. From this, it can be concluded that nitrate ions have a complexing character, and compete with Cd^{2+} for Na-DDTC.

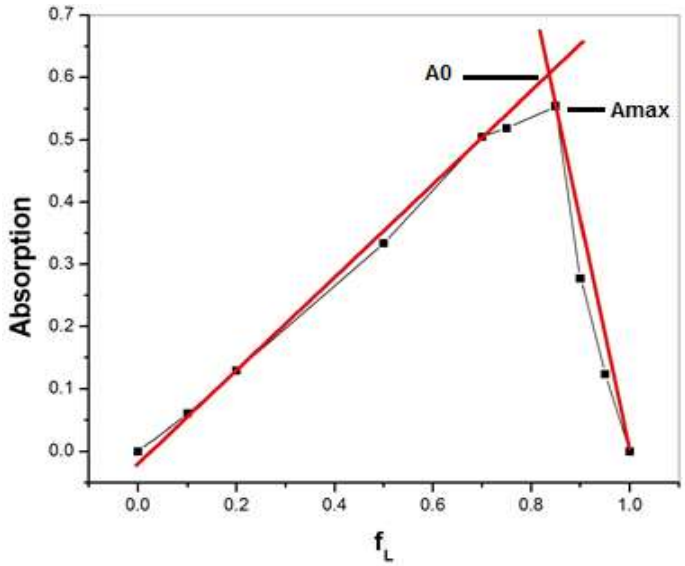

Figure 6: Job's diagram for Cd-Na-DDTC complex in 0.1 M $NaClO_4$ (λ_{max} = 300 nm).

Effect of T

Thermodynamic parameters provide information about the structure, the kind of complex, and the nature of the interaction between Na-DDTC and Cd^{2+}. These parameters were calculated using Eqs. (17-19):

$$\Delta G^0 = -RT\ lnK \quad (17)$$

$$\Delta G^0 = \Delta H° - T\Delta S° \quad (18)$$

These equations can be arranged to give Eq. (19):

$$lnK = -\frac{\Delta H°}{RT} + \frac{\Delta S°}{R} \quad (19)$$

The plot of lnK or lnβ *vs.* $\frac{1}{T}$, that was not herein reported, gave a straight line. The slope and intercept of this straight line were $\frac{\Delta H°}{R}$ and $\frac{\Delta S°}{R}$ (complexation entropy), respectively.

β, q and thermodynamic parameters of the complexation process were determined in KNO_3 or $NaClO_4$ solutions at different T (Table 7). These results show that ΔGº was negative, which confirms the spontaneous nature of the complexation process. Moreover, β values decreased with increasing T. At 323 K, q was found to be 4.

This shows that the complex's formation was strongly favored at lower T. On the other hand, ΔH^o negative values indicate an exothermic interaction between Na-DDTC and Cd^{2+}. ΔS^o positive values led to an increase in the solution, and accordingly, the complex's structure disordering. ΔS^o value in the $NaClO_4$ solution was higher than that from the KNO_3 one, showing an increase in steric factor [39]. K_f was more favored in the $NaClO_4$ solution.

Table 7: β for Cd-Na-DDTC calculated from Job's method, at various T, in $NaClO_4$ and KNO_3 solutions, with different thermodynamic parameters.

T (K)	Solution	q	α	*LogK* or logβ	$-\Delta H^0$ (kJ/mol)	ΔS^0 (J/mol)	$-\Delta G^0$ (kJ/mol)	R^2
298		5	0.096	22.26			7.693	
313	KNO_3	5	0.067	19.43	6.546	3.847	7.726	0.998
323		4	0.118	18.17			7.793	
298		6	0.057	23.94			7.872	
313	$NaClO_4$	5	0.120	21.97	5.198	7.077	8.045	0.984
323		4	0.054	18.99			8.450	

Effect of Ct

DPV showed that, even in acidic media, Cd-Na-DDTC complex was formed. For this reason, IE(%) of the complex on CS corrosion in H_2SO_4 was studied. Corrosion parameters for CS in 0.5 M H_2SO_4 were determined, from WL measurements, at different Ct (50-500 mg/L) of the studied inhibitor, at various T (Fig. 7).

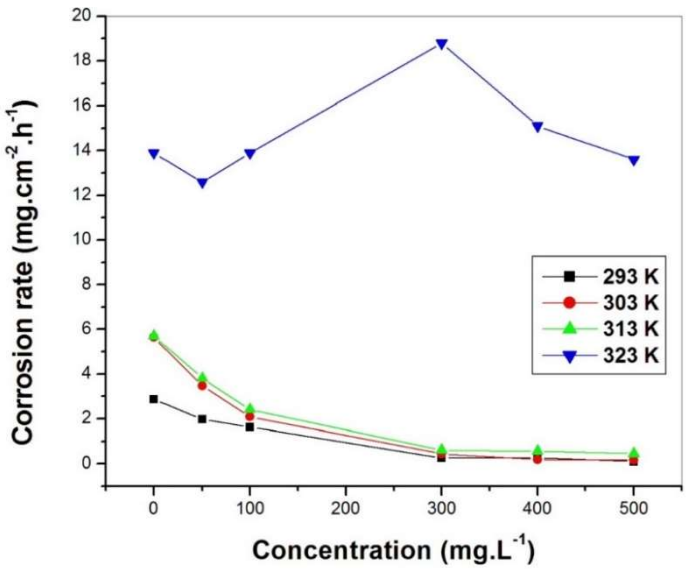

Figure 7: Relationship between CR and Na-DDTC Ct, at different T.

Fig. 7 shows that, at the initial Ct of Na-DDTC (50 mg/L), CR stayed high. Thus, this Ct was not enough to cover the entire CS's surface, and IE(%) was low. When it was increased, CR decreased for all T, except 323 K, and the inhibitor formed an effective film that protected the CS's surface. This was accompanied by a decrease in CR and an increase in IE(%), as a function of the inhibitor's Ct. Maximum IE(%) (>96) was obtained with a Ct of 500 mg/L.

Concerning general dissolution mechanism for CS, the one proposed by [40], which found that CS is positively charged in a H_2SO_4 medium, was herein adopted. SO_4^{2-} anions act as connecting bridges between protonated organic inhibitors and positively charged metal surfaces, as expressed in Eqs. (20-22).

$$Fe + SO_4^{2-} \rightarrow (FeSO_4^{2-})_{ads} \quad (20)$$

$$(Fe\ SO_4^{2-})_{ads} \leftrightarrow (Fe\ SO_4)_{ads} + 2e^- \quad (21)$$

$$(Fe\ SO_4)_{ads} \leftrightarrow Fe^{2+} + SO_4^{2-} \quad (22)$$

Furthermore, CS corrosion in H_2SO_4 solutions was an electrochemical process. The anodic reaction (Eq. 23) was:

$$Fe \rightarrow Fe^{2+} + 2e^- \quad (23)$$

And cathodic behavior corresponded to Volmer's reaction (Eq. 24):

$$H^+ + e^- \rightarrow H_{ads} \quad (24)$$

followed by Tafel's reaction (Eq. 25):

$$H_{ads} + H_{ads} \rightarrow H_2. \quad (25)$$

or Heyrovsky's reaction (Eq. 26):

$$H^+ + H_{ads} + e^- \rightarrow H_2 \quad (26)$$

Effect of T

To investigate T effect on CR, WL measurements were performed at different T (298-323 K), without and with inhibitor, at various Ct (Table 8).

Table 8: CR and IE(%) for CS in a 0.5 M H_2SO_4 solution with different Ct of Na-DDTC, at various T.

T (K)	293	303	308	323	293	303	308	323
Ct of Na-DDTC (mg/L)	CR ($mg/cm^{-2}/h$)				IE(%)			
0	2.87	5.64	5.70	13.9	-	-	-	-
50	1.97	3.47	3.80	12.6	31.35	38.47	33.33	0.096
100	1.64	2.085	2.405	13.9	42.85	63.03	57.80	0.00
300	0.260	0.445	0.61	18.8	90.94	92.10	89.29	-35.25
400	0.261	0.190	0.557	15.1	90.91	96.63	90.22	-8.63
500	0.103	0.169	0.444	13.6	96.41	97.00	92.21	2.15

Inspection of the results reveals that CR decreased with higher inhibitor's Ct. So, at 500 mg/L, IE(%) reached maximum values of 96.43, 96.98, and 92.2%, at 293, 303 and 308 K, respectively.

The fact that IE(%) decreased with higher T suggests a physical adsorption mechanism. This may be due to an increase in the solubility of the protective barrier. On the other hand, the decrease in IE(%) with higher T may also be due to a possible shift in K_{ads} towards the desorption of the adsorbed inhibitor molecules. Inversely, IE(%) increased with T from 293 to 303 K. That suggests a chemical

adsorption mechanism [41]. So, physisorption was predominant at higher T, while chemical adsorption predominated at lower ones (≤ 303 K).

Synergistic effect of Cd^{2+}

To show the effect of Cd^{2+} addition to Na-DDTC on its IE(%), the metal's Ct was increased from 4.43 to 22.53 mg/L, while the ligand's Ct was kept constant. Table 9 shows that the decrease in CR of CS in 0.5 M H_2SO_4 with Cd^{2+} was more pronounced than that without it. This table also shows that CR visibly decreased with increased Ct of Cd^{2+}. As a result, IE(%) also substantially increased. This result may be explained by Cd ions and Na-DDTC molecules co-adsorption onto the CS surface, which involved a possible increase in Cd^{2+} synergistic effect. Therefore, it was concluded that Cd-Na-DDTC complex was more hydrophobic in the CS surface, and it had low electronegativity and easy polarization in the electronic layer.

Table 9: CR and IE(%) for XC38 CS in a 0.5 M H_2SO_4 solution, at 303 K, at different Ct of Cd^{2+} with 100 mg/L Na-DDTC.

Ct from Cd^{2+} x 10^5 (mol/L)	CR x 10^5 ($g/cm^{-2}/h$)	IE(%)
0	208.5	63.03
2	2.74	80.1
4	1.87	86.6
6	1.35	90.3
10	0.0486	99.7

It is worthwhile to note that, when H_2SO_4 was added to Na-DDTC without Cd ion, the synergistic effect was not seen. Inversely, when Cd ion was added to Na-DDTC without H_2SO_4, IE(%) increased. This could mean that although H_2SO_4 can degrade Na-DDTC, it cannot dissolve the complex.

Adsorption study

Most often, organic CI act on the metal surface by adsorption. It is known that the determination of adsorption types and thermodynamic parameters serves to understand the interaction between metal surface and inhibitor.

Assuming that CI mechanism was due to Na-DDTC adsorption, according to [42], the degree of metal surface coverage (θ) was calculated from WL measurements, using Eq. (27):

$$\theta = \frac{V_{corr} - V'_{corr}}{V_{corr}} \quad (27)$$

where V_{corr} and V'_{corr} are CR for solutions without and with inhibitor, respectively. Therefore, SC was calculated using Eq. (28):

$$\theta = \frac{IE(\%)}{100} \quad (28)$$

In order to verify the suitable adsorption mode, various isotherms, including Temkin's, Frumkin's, Flory Huggins' and Langmuir's, were tested. The best fit was obtained with Langmuir's isotherm. According to it, the inhibitor Ct was related with SC by Eq. (29):

$$\frac{C_{inh}}{\theta} = \frac{1}{K_{ads}} + C_{inh} \quad (29)$$

K_{ads} denotes the interaction strength between adsorbent and adsorbate [43]. The plot of $\frac{C_{inh}}{\theta}$ *vs.* C_{inh}, at different T, yielded straight lines (Fig. 8 (A)).

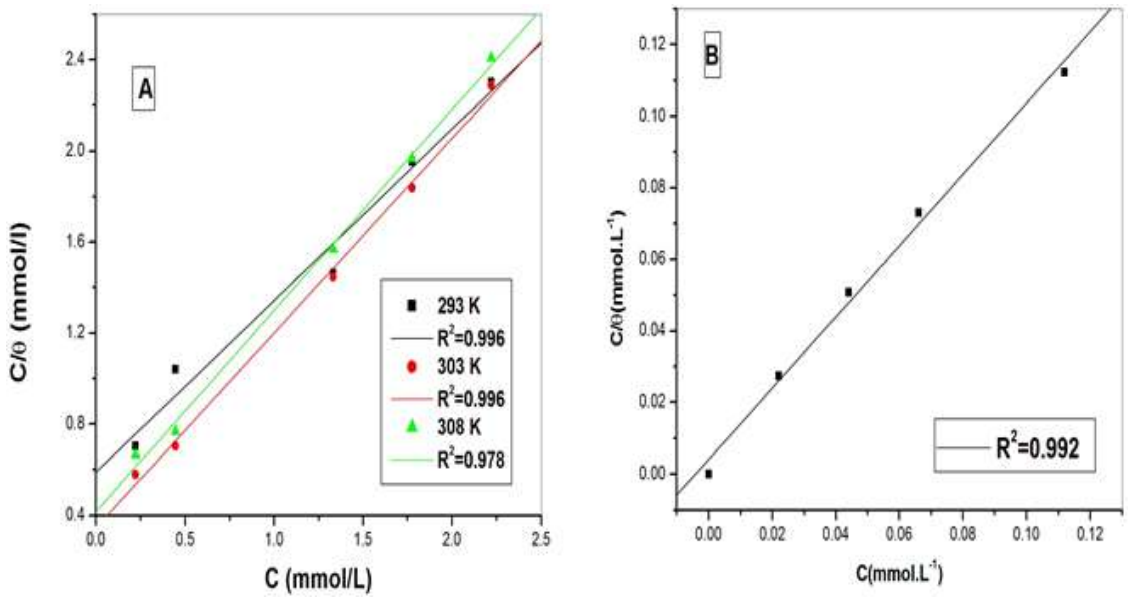

Figure 8: Langmuir's adsorption isotherm on CS in 0.5 M H_2SO_4 for- **(A)** Na-DDTC and **(B)** Cd-Na-DDTC.

Table 10 shows R^2 values and the slope of all straight lines, which were close to 1. This confirms that the inhibitor adsorption onto the CS surface obeyed Langmuir's isotherm. However, a deviation of the slopes from unity can be seen, which was due to the interaction between adsorbates on the metal surface [44-46], and to the fact that adsorption heat changed with the increasing SC [44]. So, Langmuir's isotherm could not be rigorously applied. Thus, Na-DDTC's behavior was interpreted by a modified Langmuir's isotherm, which suggested that each molecule inhibitor could occupy n's adsorbed sites [31]. This modified expression is given in Eq. (30):

$$\frac{C_{inh}}{\theta} = \frac{n}{K_{ads}} + nC_{in} \quad (30)$$

K_{ads} value obtained from the intercept enabled to calculate ΔG^{o}_{ads}, as in Eq. (31):

$$K_{ads} = \frac{1}{55.5} \exp\left(\frac{-\Delta G^{\circ}_{ads}}{RT}\right) \quad (31)$$

where 55.5 is the molar Ct of water in the solution in mol/L^{-1}.
From the intercept in Fig. 8 (A) and from Eq. (31), K_{ads} and ΔG^{o}_{ads} (Table 10) for Na-DDTC were determined at different T. K_{ads} larger value obtained at 308 K suggests that corrosion IE(%) of Na-DDTC improved at this T, leading to the formation of a protective film at the metal/solution interface, which reduced chemical attacks on CS. ΔG^{o}_{ads} negative values at all tested T revealed that the adsorption process was spontaneous.

According to [45], ΔG^{o}_{ads} values up to -20 kJ/mol^{-1} cause physisorption, while values lower than -40 kJ/mol^{-1} lead to chemisorption. In this study, ΔG^{o}_{ads} values were from -20 to -40 kJ/mol^{-1}. This suggests that Na-DDTC went through both physical and chemical adsorption [47].

The plot of $\frac{C_{inb}}{\theta}$ *vs.* C_{inh}, in Cd-Na-DDTC complex's case, was a straight line (Fig. 8 (B)) with the slope equal to unity and R^2 equal to 0,99. This confirmed that the inhibitor adsorption followed Langmuir's isotherm. The intercept gave K_{ads}, as represented in Table 10.

Table 10: Thermodynamic parameters obtained from gravimetric study for Na-DDTC and Cd-Na-DDTC adsorption onto the CS surface in 0.5 M H_2SO_4.

Solutions	T (K)	Slope	R^2	K × 10^{-3} (L/mol)	ΔG_{ads}^{0} (kJ/mol)
Na-DDTC	293	0.753	0.989	1.278	-27.21
	303	0.854	0.998	2.465	-29.79
Cd-Na-DDTC	308	0.882	0.998	2.109	-29.88
	303	1	0.992	239.808	-41.33

The obtained results indicate that K_{ads} values were higher than those obtained by Na-DDTC alone, which might be due to the presence of a strong bond between adsorbate and adsorbent. More importantly, ΔG^{o}_{ads} value for Cd-Na-DDTC complex around -40 kJ/mol led to chemisorption process. This was due to the transfer of an unshared electronic pair of organic molecules to the metal surface, thus forming a dative bond.

Synergistic effect mechanism

S_p for different Ct of Cd^{2+} in 0.5 M H_2SO_4 with 100 mg/L Na-DDTC was determined from the relationship proposed by [48] (Eqs. (32-33)).

$$S_P = \frac{1-P_{1+2}}{1-P'_{1+2}} \quad (32)$$

with

$$P_{1+2} = (P_1 + P_2) - (P_1 \times P_2) \quad (33)$$

where P_1, P_2 and P'_{1+2} are IE(%) values of Na-DDTC, Cd^{2+} and of Cd-Na-DDTC, respectively. S_p values are given in Table 11.

Table 11: S_p for different Ct of Cd^{2+} + 100 mg/L^{-1} Na-DDTC.

10^{-5}/ M [Cd^{2+}]	P_1/%	P'_{1+2}/%	P_2/%	S_P
2	7.07	80.1	63	3.4
4	18.09	86.6	63	3
6	28.77	90.3	63	2.6

It was noted that all S_p values were greater than unity. This result shows that Cd-Na-DDTC high CI on CS was due to the synergy effect. As a matter of fact, [49] explained the synergy effect either by competitive or by cooperative

adsorption between two compounds. In the first case, the two compounds are adsorbed on different sites onto the electrode surface. In the second case, one compound is chemisorbed onto the metal surface and the other is physisorbed onto it. If $S_p < 1$, thre is competitive adsorption. If $S_p > 1$, cooperative adsorption occurs. The values obtained in this study were well above unity, which shows cooperative adsorption between Na-DDTC and Cd^{2+}. Thus, the synergistic effect can be explained as follows: Na-DDTC was protonated in the acidic solution. Then, the protonated Na-DDTC and Cd^{2+} could attach onto CS through electrostatic interaction with the negatively charged surface, which was provided with the specifically adsorbed SO_4^{2-} anions onto the $FeSO_4^{2-}$ surface. When Na-DDTC adsorbed onto the CS surface, coordinate bonds were formed by the partial transference of electrons from unprotonated N and S atoms and delocalized π electrons in S atoms groups to the metal surface and to the Cd^{2+} ions, which were able to form stable complexes with the ligand. Therefore, in the adsorption process, both physical and chemical adsorption took place.

Conclusion

Experimental results indicated that Na-DDTC exhibited high propensity to form a stable complex with Cd^{2+}, in both KNO_3 and $NaClO_4$ solutions. β of the produced compound exhibited higher values in $NaClO_4$ than those of KNO_3. This was due to the competition for Cd^{2+} between NO_3^- ions and the ligand. Negative ΔG° values seen in the complexation process revealed the intrinsic spontaneity of complexation. Observed values show that ΔG° became more negative at lower T, providing evidence for the enhanced stability of the complex under these conditions. The exothermic interaction between Na-DDTC and Cd^{2+} was shown by the existence of negative ΔH° and positive ΔS values, highlighting the disorder of the complex structure. DPV and spectrophotometric measurements were in good agreement. Furthermore, Na-DDTC functioned as CI for XC38 CS, when immersed in 0.5 M H_2SO_4. An increase in the Ct from Na-DDTC enhanced IE(%), while higher T diminished it. Na-DDTC adsorbed according to Langmuir's adsorption isotherm. Thermodynamic data suggested that Na-DDTC action involved both physisorption and chemisorption processes. The synergistic impact of Cd^{2+} ions on CI by Na-DDTC was also highlighted. The chemisorption process of Cd-Na-DDTC was confirmed by measuring $\Delta G°_{ads}$ value.

Conflicts of interest

There are no conflicts of interest among the authors.

Authors' contributions

Djamila Hammoum: performed experiments; collected the data; wrote the paper. **Lahcène Larabi**: chose the problem; conceptualized ideas; supervised the whole work; wrote some sections of the manuscript. **Yahia Harek**: helped analysing results; guided in the paper writing.

Abbreviations

A: absorbance
A_0: initial absorption before dissociation

A_{ML}: absorbance value of metallic complex
$CdCl_2H_2O$: cadmium chloride
CI: corrosion inhibition/inhibitor
C_L: concentration of the ligand
C_M: metal concentration
CR: corrosion rate
CS: carbon steel
Ct: concentration
CVM: continuous variation method
DPV: differential pulse voltammetry
DTC: dithiocarbamates
E_p: peak potential
E_{pa}: anodic peak potential
E_{pc}: cathodic peak potential
F: Faraday constant
F_L: molar fraction of ligand
Fw: formula weight
H_2SO_4: sulfuric acid
HMDE: Hanging Mercury Drop Electrode
IE(%): inhibition efficiency
I_M: currents for free metal
I_{MLq}: current for complexed metal
I_{pa}: anodic peak current
I_{pc}: cathodic peak current
K_{ads}: equilibrium constant of the adsorption
Kf: formation constant of complex
KNO_3: potassium nitrate
[L]: molar concentration of ligand at equilibrium
[M]: molar concentration of the metal ion at equilibrium
[MLq]: molar concentrations of metal complex at equilibrium
$NaClO_4$: sodium perchlorate
Na-DDTC: sodium diethyldithiocarbamate tryhydrate ($C_5H_{16}NNaO_3S_2$)
q: coordination number of ligand
R: universal gas constant (8.315 $J.K^{-1}.mol^{-1}$)
R^2: linear correlation coefficient
SC: surface coverage (θ)
SE: supporting electrolyte
S_p: synergy parameter
T: absolute temperature in Kelvin (K)
WL: weight loss

Symbols definition
α: fraction of dissociation of complex
β: stability constant of the complex
n: number of electrons involved in the reaction
ΔE_p: difference between metal ion reduction and the complex peak potentials

ΔG°: standard free energy change of complexation
ΔG^{o}_{ads}: standard free enthalpy of adsorption energy
ΔH°: standard enthalpy changes of complexation
ΔS°: standard entropy changes of complexation
ε_{L}: extinction coefficient of ligand
ε_{M}: extinction coefficient of metal
γ_{L}^{q} : metal activity coefficient
γ_{M}: metal activity coefficient
$\gamma_{M\gamma_{L}^{q}}$: activity coefficient of the complex
λ_{max}: maximum wavelength

References

1. Heard PJ. Main group dithiocarbamate complexes. Prog Inorg Chem. 2005;53:1-69. https://doi.org/10.1002/0471725587.ch1
2. Adeyemi JO, Onwudiwe DC. Organotin (IV) dithiocarbamate complexes: Chemistry and biological activity. Molecules. 2018;23(10):2571. https://doi.org/10.3390/molecules23102571
3. Jamaluddin NA, Baba I, Ibrahim N. Synthesis, structural and antibacterial studies of new dithiocarbamate complexes of Sb (III) and Bi (III). Malays J Analyt Sci. 2014;(18)2:251-259.
4. Andrew FP, Ajibade PA. Metal complexes of alkyl-aryl dithiocarbamates: Structural studies, anticancer potentials and applications as precursors for semiconductor nanocrystals. J Mol Struct. 2018;1155:843-855. https://doi.org/10.1016/j.molstruc.2017.10.106.
5. Amir MK, Khan SHZ, Hayat F et al. Anticancer activity, DNA-binding and DNA-denaturing aptitude of palladium (II) dithiocarbamates. Inorg Chim Acta. 2016;451:31-40. https://doi.org/10.1016/j.ica.2016.06.036
6. Shahraki S, Mansouri-Torshizi H, Heydari A et al. Platinum (II) and Palladium (II) complexes with 1, 10-phenanthroline and pyrrolidinedithiocarbamato ligands: synthesis, DNA-binding and anti-tumor activity in leukemia K562 cell lines. Iran J Sci Technol. 2015;39(A2):187. http://ijsts.shirazu.ac.ir
7. Yin J, Miaomiao Wu, Jielin D et al. Pyrrolidine dithiocarbamate inhibits NF-KappaB activation and upregulates the expression of Gpx1, Gpx4, occludin, and ZO-1 in DSS-induced colitis. Appl biochem Biotechnol. 2015;177(8):1716-1728. https:/doi.org/10.1007/s12010-015-1848-z
8. Liddell, Jeffrey R, Lehtonen et al. Pyrrolidine dithiocarbamate activates the Nrf2 pathway in astrocytes. J Neuroinflammation. 2016;13(1):1-14. https:/doi.org/10.1186/s12974-016-0515-9
9. Abu-El-Halawa Rajab Z, Sami A. Removal efficiency of Pb, Cd, Cu and Zn from polluted water using dithiocarbamate ligands. J Taibah Univ Sci. 2017;11(1):57-65. https://doi.org/10.1016/j.tusci.2015.07.002
10. Mohd Radzi MW, Alias N AA, Esa F et al. Synthesis, characterisation and corrosion inhibition screening of Co (Ii) dithiocarbamate complexes in HCl and H_2SO_4. J Acad. 2021;9:1-10. https://ir.uitm.edu.my/id/eprint/53797

11. Hong-bo F, Hui-long W, Xing-ping G et al. Corrosion inhibition mechanism of carbon steel by sodium N, N diethyl dithiocarbamate in hydrochloric acid solution. Anti Corros Methods Mater. 2002;49(4):270-276. https://doi.org/10.1108/00035590210431782
12. Li L, Qu Q, Bai W et al. Sodium diethyldithiocarbamate as a corrosion inhibitor of cold rolled steel in 0.5 M hydrochloric acid solution. Corros Sci. 2012;59:249-257. https://doi.org/10.1016/j.corcsi.2012.03.008
13. Pham TH, Woo-Hyuk L, Gyeong-Ho S et al. Synthesis and Corrosion Inhibition Potential of Cerium/Tetraethylenepentamine Dithiocarbamate Complex on AA2024-T3 in 3.5% NaCl. Materials. 2022;15(19):6631. https://doi.org/10.3390/ma15196631
14. Kadhim MM, Juber LAA, Al-Janabi AS. Estimation of the Efficiency of Corrosion Inhibition by Zn-Dithiocarbamate Complexes: a Theoretical Study. Iraqi J Sci. 2021:3323-3335. https://doi.org/10.24996/ijs.2021.62.9(SI).3
15. Denissen PJ, Garcia SJ. Reducing subjectivity in EIS interpretation of corrosion and corrosion inhibition processes by in-situ optical analysis. Electrochim Acta. 2019;293:514-524. https://doi.org/10.1016/j.electacta.2018.10.018
16. Mohammadi I, Shahrani T, Mahdavian M et al. Cerium/diethyldithiocarbamate complex as a novel corrosion inhibitive pigment for AA2024-T3. Sci Rep. 2020;10(1):5043. https://doi.org/10.1038/s41598-020-61946-8
17. Zuman P. The Elucidation of Organic Electrode Processes: A Polytechnic Press of the Polytechnic Institute of Brooklyn Book2013: Academic Press.
18. Hanrahan G, Patil DG, Wang J. Electrochemical sensors for environmental monitoring: design, development and applications. J Environ Monit. 2004;6(8):657-664. https://doi.org/10.1039/B403975K
19. Xing X, Liu S, Yu J et al. Electrochemical sensor based on molecularly imprinted film at polypyrrole-sulfonated graphene/hyaluronic acid-multiwalled carbon nanotubes modified electrode for determination of tryptamine. Biosens Bioelectron. 2012.31(1):277-283. https://doi.org/10.1016/j.bios.2011.10.032
20. Tatsumi H, Shiba M. Polarography with a dropping carbon electrode. Electrochem Commun. 2012;20:160-162. https://doi.org/10.1016/j.elecom.2012.04.021
21. Crow DR. Polarography of metal complexes1969: Academic press London.
22. Lingane JJ. Interpretation of the Polarographic Waves of Complex Metal Ions. Chem Rev. 1941;29(1):1-35. https://doi.org/10.1021/cr60092a001
23. Kumar Y, Garg A, Pandey R. Polarographic reduction of curcumin at dropping mercury electrode. Int J Pharm. Sci. 2012;4(2):314-318.
24. Ernst R, Allen HE, Mancy KH. Characterization of trace metal species and measurement of trace metal stability constants by electrochemical techniques. 1975. https://doi.org/10.1016/0043-1354(75)90125-6

25. Heyrovský J, Ilkovič D. Polarographic studies with the dropping mercury electrode. Part II. The absolute determination of reduction and depolarization potentials. Collect Czechoslov Chem Commun. 1935;7:198-214. https://doi.org/10.1135/cccc19350198
26. Olson EJ, Bühlmann P. Getting more out of a Job's plot: determination of reactant to product stoichiometry in cases of displacement reactions and n: n complex formation. J Org Chem. 2011;76(20):8406-8412. https://doi.org/10.1021/jo201624p
27. Blanda MT, Horner JH, Newcomb M. Macrocycles containing tin. The preparation of macrobicyclic Lewis acidic hosts containing two tin atoms and tin-119 NMR studies of their chloride and bromide binding properties in solution. J Org Chem. 1989;54(19):4626-4636. https://doi.org/10.1021/jo00280a033
28. Napoli A. Complex formation of iron (III) with diglycolic and imindiacetic acids. J Inorg. Nucl Chem. 1972;34(3):987-997. https://doi.org/10/1016/0022-1902(72)80076-9
29. Boccio M, Sayago A, Asuero AG. A bilogarithmic method for the spectrophotometric evaluation of stability constants of 1: 1 weak complexes from mole ratio data. Int J Pharm. 2006;318(1-2):70-77. https://doi.org/10.1016/j.ijppharm.2006.03.026
30. Guozhen C. Ultraviolet-visible spectroscopy (Part 1). 1983, Atomic Energy Press, Beijing.
31. Villamil RF, Corio P, Agostinho S et al. Effect of sodium dodecylsulfate on copper corrosion in sulfuric acid media in the absence and presence of benzotriazole. J Electroanalyt Chem. 1999;472(2):112-119. https://doi.org/10.1016/S0022-0728(99)00267-3
32. Zarrok H, Oudda H, Zarrouk A et al. Weight loss measurement and theoretical study of new pyridazine compound as corrosion inhibitor for C38 steel in hydrochloric acid solution. Der Pharm Chem. 2011;3(6):576-590. http://derpharmachemica.com/archive.html
33. Abdulridha AA, Allah MAAH, Makki SQ et al. Corrosion inhibition of carbon steel in 1 M H_2SO_4 using new Azo Schiff compound: Electrochemical, gravimetric, adsorption, surface and DFT studies. J Mol Liq. 2020;315:113690. https://doi.org/10.1016/j.molliq.2020.113690
34. Marques A, Chierice GO. Polarographic and spectrophotometric study of lead complexes with diethanoldithiocarbamate. J Braz Chem Soc. 1998;9(6):531-538. https://doi.org/10.1590/S0103-50531998000600005
35. Çakir O, Coşkun EE, Biçer E et al. Voltammetric and polarographic studies of eriochrome black T-nickel (II) complex. Turk J Chem. 2001;25(1):33-38. https://journals.tubitak.gov.tr/chem/vol25/iss1/4
36. Nezhadali A, Langara P, Hosseini HA. Study of Complex Formation between 5, 7-Diiodo-8-hydroxyquinoline and Zn^{2+}, Cd^{2+}, Pb^{2+} and Tl^{+} Cations in Binary Non-Aqueous Solvents Using Square Wave Polarography Technique (SWP). J Chin Chem Soc. 2008;55(2):271-275. https://doi.org/10.1002/jccs.200800040

37. Thorn GD, Ludwig RA. The dithiocarbamates and related compounds. 1962.
38. Hulanicki A. Complexation reactions of dithiocarbamates. Talanta. 1967;14(12):1371-1392. https://doi.org/10.1016/0039-9140(67)80159-0
39. Al-Sarawy AA, El-Bindary AA, El-Sonbati AZ et al. Potentiometric and thermodynamic studies of 3-(4-methoxyphenyl)-5-azorhodanine derivatives and their metal complexes with some transition metals. XIV. Chem Pap. 2005;59(4):261.
40. Mohanapriya N, Kumaravel M, Lalithamani B. Theoretical and Experimental Studies on the Adsorption of N-[(E)-Pyridin-2-ylmethylidene] Aniline, a Schiff Base, on Mild Steel Surface in AcidMedia. J Electrochem Sci Technol. 2020;11(2):117-131. https://doi.org/10.33961/jecst.2019.00430
41. Gomma GK. Influence of copper cation on inhibition of corrosion for steel in presence of benzotriazole in sulfuric acid. Mater Chem Phys. 1998;55(2):131138. https://doi.org/10.1016/S0254-0584(98)00084-4
42. Ebenso EE, Obot IB. Inhibitive properties, thermodynamic characterization and quantum chemical studies of secnidazole on mild steel corrosion in acidic medium. Int J Electrochem Sci. 2010;5(12):2012-2035. https://doi.org/10.1016/S1452-3981(23)15402-2
43. Ichchou I, Larabi L, Rouabhi H et al. Electrochemical evaluation and DFT calculations of aromatic sulfonohydrazides as corrosion inhibitors for XC38 carbon steel in acidic media. J Mol Struct. 2019;1198:126898. https://doi.org/10.1016/j.molstru.2019.126898
44. Oguzie EE, Onuoha GN, Onuchukwu Al. Inhibitory mechanism of mild steel corrosion in 2 M sulphuric acid solution by methylene blue dye. Mater Chem Phys. 2005;89(2-3):305-311. https://doi/10.1016/j.matchemphys.2004.09.004
45. Oguzie EE, Okulue BN, Ebenso EE et al. Evaluation of the inhibitory effect of methylene blue dye on the corrosion of aluminium in hydrochloric acid. Mater Chem Phys. 2004;87(2-3):394-401. https://doi.org/10.1016/j.matchemphys.2004.06.003
46. Oguzie EE. Influence of halide ions on the inhibitive effect on congo red dye on the corrosion of mild steel in sulfuric acid solution. Mater Chem Phys. 2004;87(1):212-217. https:// doi.org/10.1016/j.matchemphys.2004.06/006
47. Yurt A, Ulutas S, Dal H. Electrochemical and theoretical investigation on the corrosion of aluminium in acidic solution containing some Schiff bases. Appl Surf Sci. 2006;253(2):919-925. https://doi.org/10.1016/j.apsusc.2006.01.026
48. Aramaki K, Hackerman N. Inhibition mechanism of medium-sized Polymethyleneimine. J Electrochem Soc. 1969;116(5):568-574. https//doi: 10.1149/1.2411965.
49. Aramaki, K. Synergistic inhibition of zinc corrosion in 0.5 M NaCl by combination of cerium (III) chloride and sodium silicate. Corros Sci. 2002;44(4):871-886. https//doi:10.1016/S0010-938X(01)00087-7